Molecular Dynamics Study on the Wetting Transition of a Hierarchical Groove

Zhengqing Zhang,[†] Sungwook Chung,[‡,*] and Joonkyung Jang[†,*]

[†]*Department of Nanoenergy Engineering, Pusan National University, Busan 46241, Republic of Korea. *E-mail: jkjang@pusan.ac.kr*
[‡]*School of Chemical and Biomolecular Engineering, Pusan National University, Busan 46241, Republic of Korea. *E-mail: sungwook.chung@pusan.ac.kr*
Received November 3, 2017, Accepted December 22, 2017, Published online February 2, 2018

Keywords: Wetting, Dewetting, Restrained molecular dynamics, Superhydrophobic, Hierarchical

Superhydrophobic surfaces have extremely wide applications including anti-icing,[1] anti-frosting,[2] biological materials,[3] and water collection.[4,5] A typical superhydrophobic surface exhibits a water contact angle (CA) above 150°, a sliding angle (SA), and a contact angle hysteresis (CAH) below 10°.[6,7]

Most superhydrophobic surfaces are constructed by either embossing or engraving arrays of hierarchical micro-/nanogrooves on a flat surface. When a water droplet is deposited on such a grooved surface, the micro- and nanogrooves can be dewetted or wetted by the droplet, giving rise to the so-called Cassie–Baxter (CB)[8] or Wenzel (WZ)[9] states. There can be in principle four possible composite states for a dual-scale groove: CB–CB, CB–WZ, WZ–CB, and WZ–WZ states.[10] These composite states can be tuned from one state into another by changing the physical and chemical properties of the hierarchical structures.[10,11]

Superhydrophobic surfaces with self-cleaning properties (lotus effect) are frequently achieved by controlling the surface morphology so that both the major and minor grooves are maintained in the CB state.[10] However, the liquid–gas interfaces are subject to instability caused by an external stimulus, leading to CB to WZ (wetting) and WZ to CB (dewetting) transitions.[12] These transitions are not always instantaneous and may occur on variable time scales, occasionally giving intermediate states between the CB and WZ states. Although some progress has been made in capturing the wetting transitions of single-scale grooves using experiment and simulation,[13–15] the wetting transition mechanisms for hierarchical grooves are still unclear, especially the role of minor grooves in the wetting and dewetting transitions.

Herein, using a restrained molecular dynamic (RMD) simulation, we investigated rectangular trenches that have major and minor grooves with depths D and d and widths W and w, respectively. We study how the wetting and dewetting transitions are affected by the *depth ratio*, $d^* = d/D$, by calculating the free energy profile of the wetting. A detailed description of the RMD simulation and free energy calculation can be found in our previous work.[16] Note that the definition of filling level Z is

$$Z = \frac{N - N_{CB}}{N_{WZ} - N_{CB}} \quad (1)$$

where N is a series of target values, N_{CB} and N_{WZ} are the number of water molecules inside the collective variable (CV) cell in the CB and WZ states, respectively.

Figure 1 shows how water penetrates into a hierarchical groove with increasing the filling level of the groove, Z (which ranges from 0 to 1). As Z increases from 0.00 (CB state) to 0.28, the liquid–gas interface develops a meniscus while pinned at the top of the groove. The curvature of the meniscus gradually increases as Z changes from 0.28 to 0.82. Note also that the liquid–gas interface becomes depinned as Z is changed from 0.50 to 0.82. Eventually, the liquid–gas interface touches the bottom of the groove at $Z = 1.00$, resulting in the WZ state. During the entire wetting transition, the liquid–gas interface is symmetric, which is in agreement with the wetting transition found for a surface engraved with cylindrical pores.[13]

Plotted in Figure 2 (top) are the free energy profiles of the wetting transitions of hierarchical grooves with various depth ratios. The potential of mean force (PMF) was calculated versus Z by fixing w^* to 0.233. With an increase in Z from 0 (CB state), the PMFs increase and culminate at the transition states marked by the different symbols. With a further increase in Z, the PMFs decrease to a local minimum ($Z = 1.0$, WZ state). The density profiles of the transition states show that the minor grooves always remain in the CB states (inset of Figure 2, top). In the bottom of Figure 2, we calculated and plotted the free energy barriers of the CB to WZ (filled squares) and WZ to CB (empty squares) transitions. With increasing d^*, the free energy barriers of the CB to WZ (wetting) and WZ to CB (dewetting) transitions increase and decrease, respectively. The wetting and dewetting transitions at $d^* = 0.88$ have the highest and lowest free energy barriers, respectively. Compared with the single-scale groove, $d^* = 0.0$, the free energy barriers for the wetting and dewetting transitions significantly increase (by $9.8k_BT$) and decrease (by $1.4k_BT$). This arises from the fact that the liquid–solid (gas–solid) interface area decreases (increases), giving rise

[Correction added on 12 February 2018, after first online publication: email address of the author Sungwook Chung has been corrected].

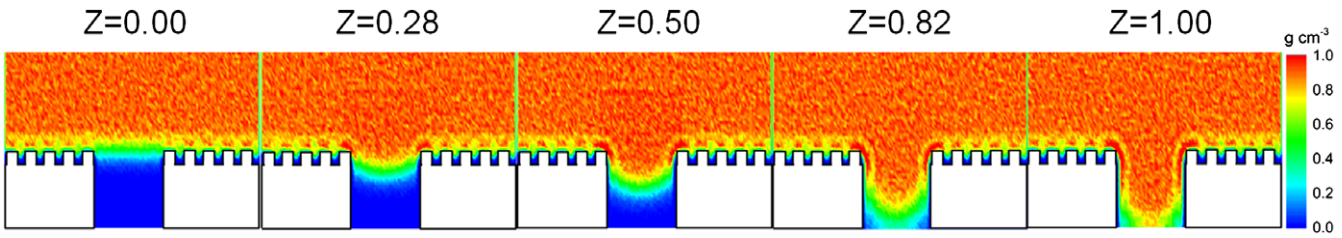

Figure 1. The wetting (CB to WZ) transition of a hierarchical groove. Shown is the average water density versus the filling level Z of the groove for $d^*(=d/D) = 0.13$ and $w^*(=w/W) = 0.233$. The same color bar is used for all the figures.

to an increased hydrophobicity of surface.[10,17] The density profiles are shown for the stable CB states in the bottom of Figure 2 (inset). Note that, with an increase in d^*, the layers of water near the top and sides of the major grooves disappear gradually by changing from *a* to *d*. This is consistent with the previous molecular dynamics simulation of the hydrophobic surface texturized with rectangular pillars.[18] The present simulation focuses on how the wetting and dewetting transitions are affected by the depth ratio. The effects of the width ratio ($w^* = w/W$) on the wetting transition and surface hydrophobicity are left as future work. Qualitatively however, we deduce that the wetting transition capability and surface hydrophobicity increase and decrease, respectively,[16–18] with increasing the width ratio.

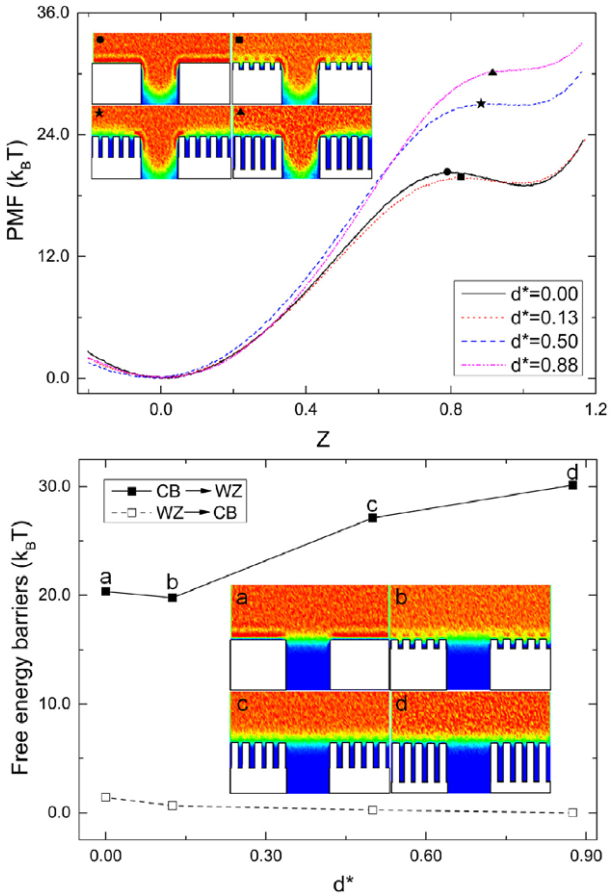

Figure 2. Free energy profiles and barriers of the wetting and dewetting transitions of hierarchical grooves. Plotted are PMF versus Z (top) and the free energy barrier versus d^* (bottom). The depth ratio, d^*, was varied as 0.0, 0.13, 0.50, and 0.88 by fixing the width ratio w^* to 0.233. The density profiles of water at the transition (top) and the stable CB (bottom) states are shown in insets.

In conclusion, we observed the symmetric liquid–gas interfaces of water in the wetting transition of rectangular hierarchical grooves. From the construction of free energy profiles, we show that the wetting transition is significantly hampered and therefore the hydrophobicity of the surface is enhanced by increasing the ratio of the depths of the minor and major grooves.

Acknowledgments. This work was supported by the Financial Supporting Project of Long-term Overseas Dispatch of PNU's Tenure-track Faculty, 2016.

References

1. C. Stamatopoulos, J. Hemrle, D. Wang, D. Poulikakos, *ACS Appl. Mater. Interfaces* **2017**, *9*, 10233.
2. W. Zhang, S. Wang, Z. Xiao, X. Yu, C. Liang, Y. Zhang, *Langmuir* **2017**, *33*, 8891.
3. Z. Wang, H. Zuilhof, *Langmuir* **2016**, *32*, 6310.
4. M. Wang, Q. Liu, H. Zhang, C. Wang, L. Wang, B. Xiang, Y. Fan, C. F. Guo, S. Ruan, *ACS Appl. Mater. Interfaces* **2017**, *9*, 29248.
5. R. Wen, Z. Lan, B. Peng, W. Xu, R. Yang, X. Ma, *ACS Appl. Mater. Interfaces* **2017**, *9*, 13770.
6. X. Zhang, F. Shi, J. Niu, Y. Jiang, Z. Wang, *J. Mater. Chem.* **2008**, *18*, 621.
7. L. Cao, T. P. Price, M. Weiss, D. Gao, *Langmuir* **2008**, *24*, 1640.
8. A. Cassie, S. Baxter, *Trans. Faraday Soc.* **1944**, *40*, 546.
9. R. N. Wenzel, *Ind. Eng. Chem.* **1936**, *28*, 988.
10. Z.-H. Yang, F.-C. Chien, C.-W. Kuo, D.-Y. Chueh, P. Chen, *Nanoscale* **2013**, *5*, 1018.
11. M. Zhang, S. Feng, L. Wang, Y. Zheng, *Biotribology* **2016**, *5*, 31.
12. F. Guo, Z. Guo, *RSC Adv.* **2016**, *6*, 36623.
13. P. Lv, Y. Xue, H. Liu, Y. Shi, P. Xi, H. Lin, H. Duan, *Langmuir* **2015**, *31*, 1248.
14. A. M. Miqdad, S. Datta, A. K. Das, P. K. Das, *RSC Adv.* **2016**, *6*, 110127.
15. Y. He, Q. Zhou, S. Wang, R. Yang, C. Jiang, W. Yuan, *Langmuir* **2017**, *33*, 3949.
16. Z. Zhang, M. Y. Ha, J. Jang, *Nanoscale* **2017**, *9*, 16200.
17. D. Zhu, W. Qiao, L. Wang, *Chin. Sci. Bull.* **2011**, *56*, 1623.
18. Z. Zhang, H. Kim, M. Y. Ha, J. Jang, *Phys. Chem. Chem. Phys.* **2014**, *16*, 5613.

